

# Mutational dynamics of influenza A viruses: a principal component analysis of hemagglutinin sequences of subtype H1

Yves-Henri Sanejouand  
UFIP, UMR 6286 of CNRS,  
Faculté des Sciences et des Techniques, Nantes, France.  
Yves-Henri.Sanejouand@univ-nantes.fr

(Dated: October 4, 2017)

PACS numbers: 87.14.E-, 87.15.Qt, 87.19.xd

Keywords: principal component analysis – multiple sequence alignment – hydrophobicity scale – hemagglutinin – influenza – pandemic

## Abstract

A principal component analysis of a multiple sequence alignment of hemagglutinin sequences of subtype H1 has been performed, the sequences being encoded using the amino-acid property that maximizes the weight of the major component. In the case of this alignment, it happens to be a well-known hydrophobicity scale. Interestingly, sequences coming from human have large positive amplitudes along the major component before 2009, and large negative ones afterwards. This means that the 2009 pandemic was associated to a major change in the hydrophobicity pattern of hemagglutinin.

The present analysis also highlights the high variability of viral sequences coming from swine. At a more general level, the method proposed in this paper allows to describe a sequence coming from an alignment with a set of numbers, the original point being that the choice of the corresponding property is driven by the data. This approach should allow the application of numerous methods to the study of large multiple sequence alignments.

## Introduction

Because it does not require any assumption about the underlying population genetic model, and also because it allows to study large datasets at a negligible computational cost, principal component analysis (PCA) [1] has been used for long for analyzing multiple sequence alignments (MSA) [2–6].

To this end, since PCA deals with numerical quantities, each sequence symbol needs to be associated to a set of numbers. In the case of nucleic acids, an obvious choice is a binary code [3, 5] where, for instance,  $\{1, 0, 0, 0\}$  corresponds to adenine,  $\{0, 1, 0, 0\}$  to cytosine, *etc.*

For proteins, because there are twenty common amino-acid residues, doing so would yield extremely sparse matrices, since many residues are never observed at a given position, even in the case of large alignments, like the one considered in the present study. This issue has for instance been addressed by using instead frequencies of amino-acid residues, in whole genomes [7], or counts of pairs of residues found in each considered sequence [2]. In the present study, it is addressed by associating a single numerical property to each residue, the property being chosen among the 544 properties gathered in the amino acid index database [8, 9], so that the relative weight of the major component of the PCA is the largest.

As a first application, this approach is used for analyzing the MSA of influenza A hemagglutinin sequences belonging to subtype H1. Gaining a better understanding of the mutational dynamics of this subtype may indeed prove of particular importance, since it has been involved in several pandemics, noteworthy the 1918-1919 one [10], which killed at least 50 million people [11], but also in the latest one, in 2009-2010 [12, 13].

## Methods

### Multiple sequence alignment

17688 hemagglutinin (HA) sequences of subtype H1 were retrieved [28] from the NCBI influenza virus resource [14], sequences coming from laboratory viral strains being disregarded, as well as redundant ones. Since obtaining an accurate MSA of a large number of sequences can prove challenging [16–18], and because H1 sequences have high levels of sequence identities, being at least 75% identical to each other [15], like in a previous study [15], pairwise alignments were performed, with BLAST [19] version 2.2.19, taking as query the long H1 sequence of virus A/Thailand/CU-MV10/2010 (genbank accession number HM752477). MVIEW [20], version 1.60.1, was then used for converting the BLAST output into an actual MSA.

Including gaps, this MSA is 575 residues long. For performing PCA, 205 sites were considered, those with little variability being disregarded, namely, all sites where the same amino-acid residue is found in at least 99% of the sequences, as well as those that are not observed in crystal structure 4EEF [21], the latter being mostly at both ends of the MSA [29].

The 4EEF structure was used for illustrative purposes, as well as for residue numbering which is, like in most available crystal structures [30], the H3 numbering, even though 4EEF is a structure of the 1918 HA, from strain A/South Carolina/1/1918 [10] (genbank accession number AF117241.1).

Though the rate of evolution of H1 sequences over the last century has not been spectacular, contemporary sequences being on average more than 80% identical to the 1918-1919 sequences [15], note that, due to the large number of H1 sequences taken into account, the variability of the 205 retained sites is high,  $\approx 10$  different residues being observed at each site of the MSA, on average.

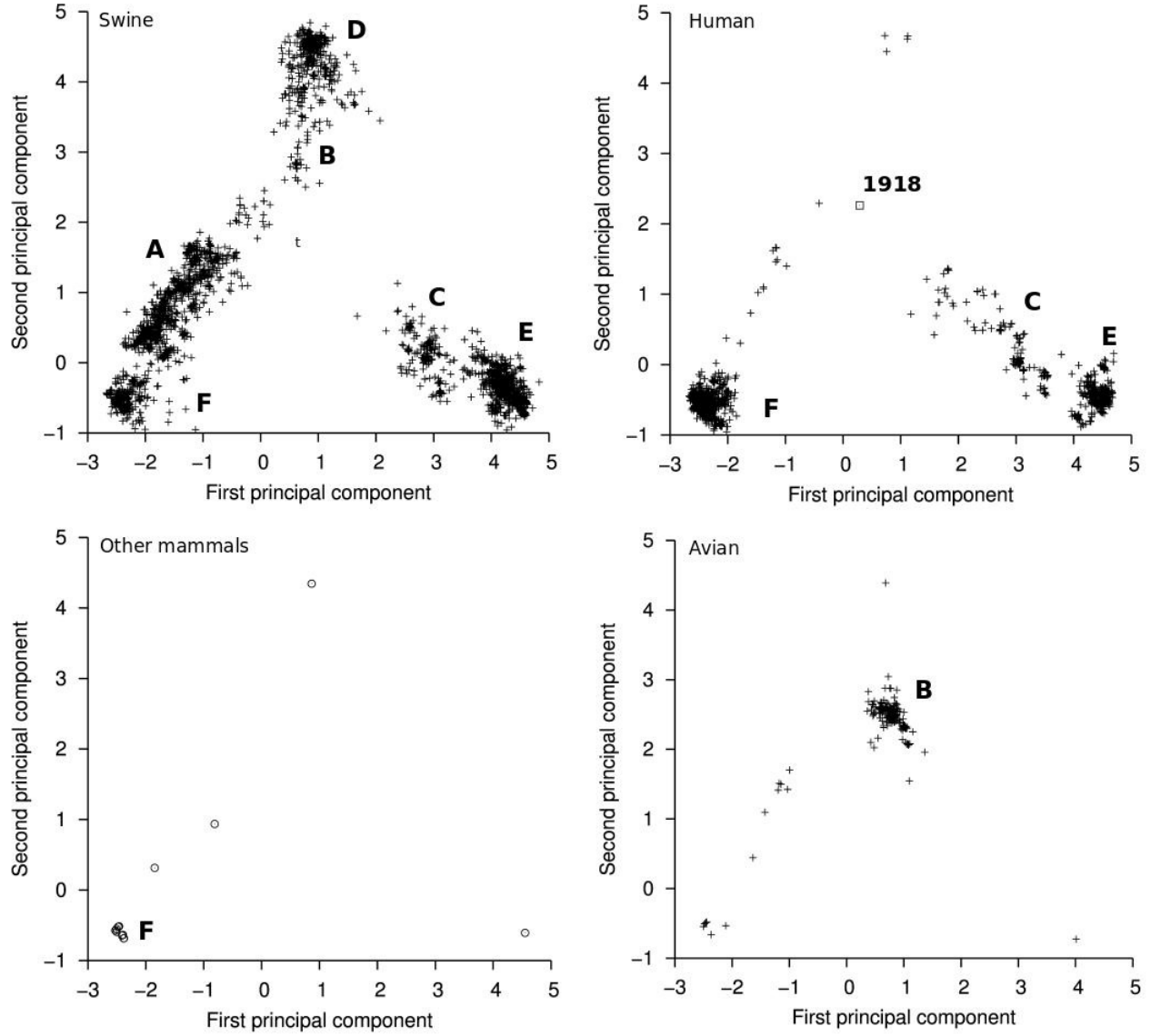


FIG. 1: *Projections of HA sequences on the two first PCA components.* Sequences come from swine (top left), human (top right), birds (bottom right) or from mammals other than swine and human (bottom left). Main sequence clusters are labelled **A-F**. Open square: the 1918 sequence.

### Principal component analysis

Let us associate a set of  $n$  numerical properties to a given residue  $i$ ,  $p_{i,1}, \dots, p_{i,n}$ , so that a sequence  $k$  of length  $N$  can be described as a vector  $\mathbf{s}_k = \{p_{1,1}, \dots, p_{N,n}\}$  of dimension  $d = nN$ . A MSA can then be described as a matrix:

$$\mathbf{S} = \begin{pmatrix} \mathbf{s}_1 - \mathbf{s}_{ref} \\ \vdots \\ \mathbf{s}_k - \mathbf{s}_{ref} \\ \vdots \\ \mathbf{s}_m - \mathbf{s}_{ref} \end{pmatrix}$$

where  $\mathbf{s}_{ref}$  is a reference sequence and  $m$ , the number of sequences.  $\mathbf{C}$ , the covariance matrix, of dimension  $d \times d$ , is:

$$\mathbf{C} = \frac{1}{m} \mathbf{S}^T \mathbf{S}$$

$\mathbf{A}$ , the orthogonal matrix with the principal components, and  $\mathbf{\Lambda}$ , the diagonal matrix with their weights, are obtained by diagonalizing  $\mathbf{C}$  [22]:

$$\mathbf{A}^T \mathbf{C} \mathbf{A} = \mathbf{\Lambda}$$

Note that the weight of a principal component gives the proportion of the variance of the sequences, with respect to the reference one, that is captured by the component.

On the other hand, since the principal components form a basis set, sequence  $k$  can be described as a set of amplitudes (projections) along the principal components:

$$q_i = \mathbf{a}_i \cdot (\mathbf{s}_k - \mathbf{s}_{ref}) \quad (1)$$

where  $q_i$  is the amplitude of sequence  $k$  along component  $i$ ,  $\mathbf{a}_i = \{a_{1,i}, \dots, a_{d,i}\}$  being the  $i^{\text{th}}$  component, that is, the  $i^{\text{th}}$

eigenvector of  $\mathbf{C}$ , and  $a_{j,i}$  the coefficient of component  $i$  for the  $j^{\text{th}}$  property of sequence  $k$  [31].

Hereafter, the  $n = 1$  case is considered and the reference sequence, for which  $\mathbf{q} = \mathbf{0}$ , is the average sequence of the MSA. Gaps and unknown residues are treated as follows: the property value of a gap is assumed to be the average value at the considered site; the property value of an unknown residue is assumed to be the value obtained for the closest sequence having a known residue at that site.

Projections (eqn 1) were only performed for long enough sequences, namely, for the 11869 sequences where a known amino-acid residue is found in at least 90% of the 205 selected sites of the MSA.

## Results

### Choice of the amino-acid property

All 544 properties of the amino acid index database [8, 9] were tried one after the other, a PCA of the MSA with the 17688 H1 sequences being performed for each of them. The weight of the major (first) component varies between 39.9% and 63.9% of the overall variance (the trace of  $\mathbf{C}$ ) of the sequence dataset. Interestingly, properties yielding the largest weight for the major component are well known hydrophobicity scales. Indeed, the scales that are, according to our criterion, the three best ones were built with residue contact matrices [25], mean polarities [24] and amino-acid partition energies [23].

Being the best one, the former was retained for further analysis. It corresponds to the following residue ranking: EKRS-DQGNPHTAMWYCFLVI. As expected for an hydrophobicity scale, the two basic (RD) and the two acidic (ED) residues are at one end of the scale, namely, among the five first ones, while the four last ones (FLVI) are the residues that are the most often considered to be the most hydrophobic ones [26]. The weights of the second and third components are 9.8% and 3.5%, respectively. Thus, nearly three quarters (74%) of the fluctuations of the 17688 H1 sequences can be described with two components *only* (among 205), most remaining ones being of little significance. As a matter of fact, only eight components have a weight of more than 1%.

### Projections on the two first components

Sequence fluctuations are, by definition [22], the largest along the major component. As shown in Figure 1, where the projections of H1 sequences on the two major components (eqn 1) are plotted, most human sequences (Figure 1, top right) belong to a pair of clusters, coined **E** and **F**, which correspond to extreme values of the amplitude along the major component:  $q_1 \approx 4.5$  and  $q_1 \approx -2.5$ , respectively. Both clusters are also observed with swine sequences (Figure 1, top left), while most sequences from mammals other than swine and human (Figure 1, bottom left) belong to cluster **F**. Note that this latter point is likely to be a consequence of the lack of data for these species before 2009. Indeed, the single sequence found in cluster **E**, from a giant anteater, was obtained in 2007 while the only other sequence obtained before 2009, from a ferret, belongs to yet another one, coined **A**. A sequence belonging to cluster **D** was also found in 2013, coming from a wild boar.

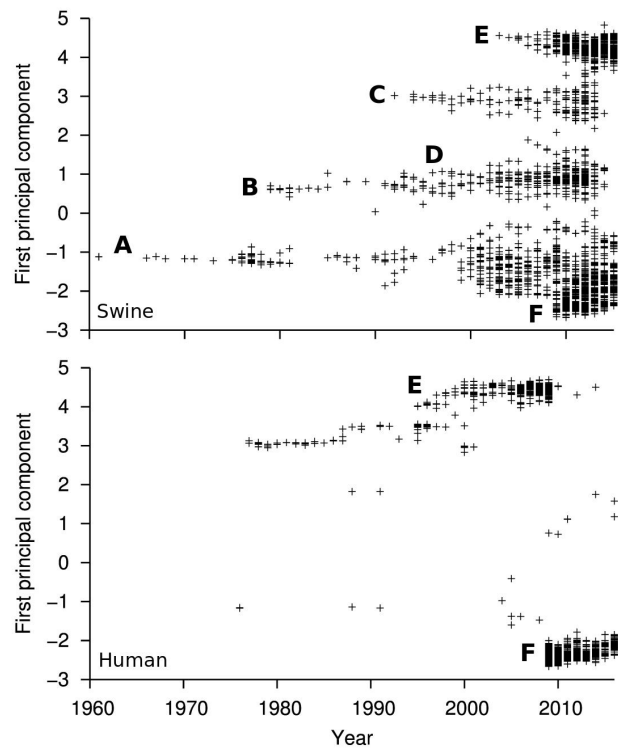


FIG. 2: Projections of HA sequences on the major PCA component, as a function of time. Sequences come from swine (top) or human (bottom). The year correspond to the collection date of each sequence, as provided by the NCBI influenza virus resource. Main sequence clusters are labelled A-F, like in Figure 1. Following the amplitude of the second component (not shown) allows to pinpoint when cluster **D** popped up.

Most avian sequences (93% of them) belong to a fourth cluster (Figure 1, bottom right), coined **B**. Since complete avian sequences are known since 1979 [32], this result confirms that a strong evolutionary pressure is at work in avian species [15], which limits the variability of avian H1 sequences.

Interestingly, the 1918 sequence colocalizes with cluster **B** (Figure 1, top right), further supporting the hypothesis of an avian origin for the 1918-1919 pandemic [10]. However, seven sequences coming from swine with collection dates between 1931 and 1942 are also located close to the 1918 sequence. Since these latter sequences are also the closest ones in terms of sequence identity [15], based on our sole analyses of the hemagglutinin sequences, the hypothesis that the 1918 virus actually came from swine would be more likely.

The limited variability of avian sequences helps highlighting a key result of the present analysis, namely, the spectacular variability of sequences coming from swine (Figure 1, top left). On the one hand, swine sequences are found in all major clusters observed with sequences of other species. On the other hand, two clusters (**A** and **D**) are mostly populated by sequences coming from swine.

## Projection as a function of time

Figure 2 shows the evolution of the projections of the sequences on the major component, as a function of their collection date. For sequences coming from swine, this analysis highlights two striking features: first, a new cluster of swine sequences has been popping up every five-ten years (lately: **E** in 2003, **F** in 2009). Second, half of them seem to have vanished after 2014 (clusters **B-D**).

For sequences coming from human, our analysis highlights the fact that, a given year, almost all of them belong to a given cluster, with a switch from cluster **E** to cluster **F** occurring in 2009. Indeed, before the 2009 pandemic, no sequence belonging to cluster **F** was found while, after 2009, sequences belonging to cluster **E** are rare (see Figure 2). On the other hand, the fact that the cluster the closest to cluster **F** is cluster **A** (see Figure 1) suggests that the former derives from the later, that is, since most sequences of cluster **A** come from swine, it supports the hypothesis that the 2009 pandemic has its origin in this species [13].

Sequences with a collection date before 1960 are rare. As a consequence, following their projections on the first component (not shown) does not allow to check if, for instance, sequences coming from human have experienced other jumps from a sequence cluster to another, like the 2009 one. This seems however likely since, while for the 1918 sequence  $q_1 \approx 0.2$ , it was significantly higher in the thirties ( $q_1$  in the 1.5–2 range).

## Analysis of the major component

Figure 3 shows that the coefficients of the major component are much larger (whatever their sign) on the head of hemagglutinin (residues 53-269), where the binding site of the receptor stands. Indeed, on the rest of hemagglutinin (86 analyzed sites) the absolute value of the coefficient is always less than 0.16 while, on the head of hemagglutinin, it is larger for 14 residues, raising up to 0.25 [33].

Moreover, six of these residues have positive coefficients, namely, A103I, T155V, A169I, S203F, K219I, N269I, the coefficients being negative for the other eight ones, namely, L53K, L78S, I80S, V133N, L160S, I188T, V205G, I244T, the residue given first being the most commonly found one before 2009 in sequences of human origin, while the second is the most commonly found afterwards [34]. This means that, though the overall hydrophobicity of the head of hemagglutinin has not changed significantly in 2009, the hydrophobicity pattern there has changed dramatically.

I188T, the residue with the third largest coefficient (in terms of absolute values), was a glycine in the 1918 HA sequence. Interestingly, at variance with all the other residues of the 1918 sequence, Gly 188 has not been observed again in H1 sequences of human origin [15]. This suggests that mutations at this position may play a key role in the development of pandemics. It further calls for a dedicated monitoring of such mutations.

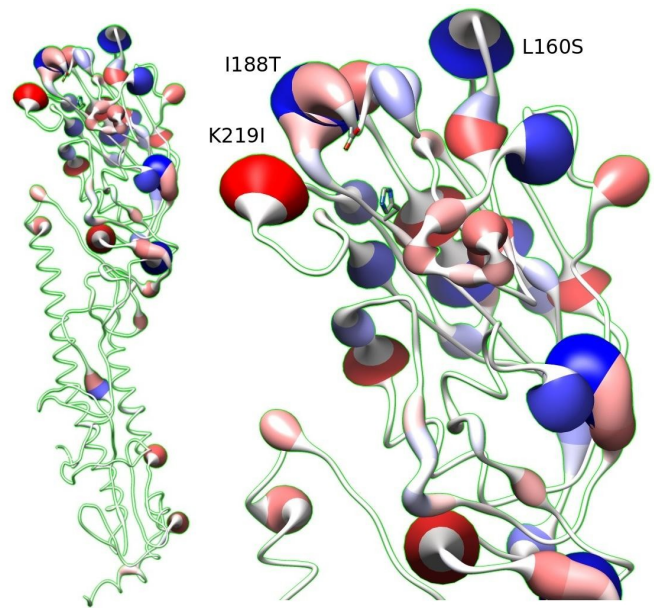


FIG. 3: *Change in the hydrophobicity pattern of hemagglutinin.* The width of the worm is proportional to the absolute value of the coefficient of the major PCA component for the residue. The colour gives the sign of the coefficient. Red means that the residue was polar before 2009 and has been hydrophobic since then. Blue means the opposite. The three residues with large absolute coefficients that are the closest to the receptor binding site are labelled, the residue the most often observed in sequences of human origin before 2009 being mentioned first, the residue the most often observed since then being mentioned last. Drawn with UCSF Chimera (version 1.11.2) [27].

## Conclusion

Encoding the hemagglutinin sequences belonging to subtype H1 with the hydrophobicity of their residues, using a well known scale [25], allows to describe  $\approx 64\%$  of the fluctuations of these sequences with a single principal component, which corresponds to a major change in the pattern of hydrophobicity on the head of hemagglutinin (Fig. 3), where the receptor binding site stands. This change occurred in 2009 (Fig. 2), suggesting that it is involved in the pandemic, probably by modifying extensively the antigenicity of hemagglutinin, thus helping the virus to escape recognition by the immune system. Taken together, the two major components allow to delineate several clusters of sequences (Fig. 1), highlighting the reduced variability of sequences of avian origin, most of them being included in a single cluster, in contrast with sequences from swine, which are found in in at least six different ones.

Projecting the swine sequences on the major component as a function of time (Fig. 2) shows that, while new clusters appear regularly, namely, every five-ten years, several seem to have vanished after 2014. As a consequence, most actual sequences from swine belong to the same two clusters where sequences of human origin are found.

In the case of hemagglutinin sequences, describing sequences with a single property per residue proved enough for getting meaningful components. It is likely that for other alignments using more properties per residue could prove helpful.

- [1] Ringnér, M (2008) What is principal component analysis? *Nature biotechnology* 26:303.
- [2] Van Heel, M (1991) A new family of powerful multivariate statistical sequence analysis techniques. *Journal of molecular biology* 220:877–887.
- [3] Casari, G, Sander, C, Valencia, A (1995) A method to predict functional residues in proteins. *Nature structural biology* 2:171.
- [4] Vinga, S, Almeida, J (2003) Alignment-free sequence comparison: a review. *Bioinformatics* 19:513–523.
- [5] Clamp, M, Cuff, J, Searle, SM, Barton, GJ (2004) The Jalview java alignment editor. *Bioinformatics* 20:426–427.
- [6] Cocco, S, Monasson, R, Weigt, M (2013) From principal component to direct coupling analysis of coevolution in proteins: Low-eigenvalue modes are needed for structure prediction. *PLoS Comput Biol* 9:e1003176.
- [7] Suhre, K, Claverie, JM (2003) Genomic correlates of hyperthermostability, an update. *Journal of Biological Chemistry* 278:17198–17202.
- [8] Kawashima, S, Kanehisa, M (2000) Aaindex: amino acid index database. *Nucleic acids research* 28:374–374.
- [9] Kawashima, S et al. (2008) AAindex: amino acid index database, progress report 2008. *Nucleic acids research* 36:D202–D205.
- [10] Reid, AH, Fanning, TG, Hultin, JV, Taubenberger, JK (1999) Origin and evolution of the 1918 "spanish" influenza virus hemagglutinin gene. *Proceedings of the National Academy of Sciences* 96:1651–1656.
- [11] Johnson, NP, Mueller, J (2002) Updating the accounts: global mortality of the 1918-1920 "spanish" influenza pandemic. *Bulletin of the History of Medicine* 76:105–115.
- [12] Smith, GJ et al. (2009) Origins and evolutionary genomics of the 2009 swine-origin H1N1 influenza A epidemic. *Nature* 459:1122–1125.
- [13] Neumann, G, Noda, T, Kawaoka, Y (2009) Emergence and pandemic potential of swine-origin H1N1 influenza virus. *Nature* 459:931–939.
- [14] Bao, Y et al. (2008) The influenza virus resource at the national center for biotechnology information. *Journal of virology* 82:596–601.
- [15] Sanejouand, YH (2017) A singular mutation in the hemagglutinin of the 1918 pandemic virus. *Archives of biochemistry and biophysics* 625:13–16.
- [16] Thompson, JD, Linard, B, Lecompte, O, Poch, O (2011) A comprehensive benchmark study of multiple sequence alignment methods: current challenges and future perspectives. *PLoS one* 6:e18093.
- [17] Sievers, F, Dineen, D, Wilm, A, Higgins, DG (2013) Making automated multiple alignments of very large numbers of protein sequences. *Bioinformatics* 29:989–995.
- [18] Chang, JM, Di Tommaso, P, Notredame, C (2014) Tcs: a new multiple sequence alignment reliability measure to estimate alignment accuracy and improve phylogenetic tree reconstruction. *Molecular Biology and Evolution* 31:1625–1637.
- [19] Altschul, SF et al. (1997) Gapped blast and psi-blast: a new generation of protein database search programs. *Nucleic acids research* 25:3389–3402.
- [20] Brown, NP, Leroy, C, Sander, C (1998) Mview: a web-compatible database search or multiple alignment viewer. *Bioinformatics* 14:380–381.
- [21] Whitehead, TA et al. (2012) Optimization of affinity, specificity and function of designed influenza inhibitors using deep sequencing. *Nature biotechnology* 30:543–548.
- [22] Rao, CR (1964) The use and interpretation of principal component analysis in applied research. *Sankhyā: The Indian Journal of Statistics, Series A* pp 329–358.
- [23] Miyazawa, S, Jernigan, RL (1999) Self-consistent estimation of inter-residue protein contact energies based on an equilibrium mixture approximation of residues. *Proteins: Structure, Function, and Bioinformatics* 34:49–68.
- [24] Radzicka, A, Pedersen, L, Wolfenden, R (1988) Influences of solvent water on protein folding: free energies of solvation of cis and trans peptides are nearly identical. *Biochemistry* 27:4538–4541.
- [25] Bastolla, U, Porto, M, Roman, HE, Vendruscolo, M (2005) Principal eigenvector of contact matrices and hydrophobicity profiles in proteins. *Proteins: Structure, Function, and Bioinformatics* 58:22–30.
- [26] Trinquier, G, Sanejouand, YH (1998) Which effective property of amino acids is best preserved by the genetic code? *Prot. Eng.* 11:153–169.
- [27] Pettersen, EF et al. (2004) UCSF chimera: a visualization system for exploratory research and analysis. *Journal of computational chemistry* 25:1605–1612.
- [28] On September 6<sup>th</sup>, 2016.
- [29] There are 498 amino-acid residues in each HA monomer of 4EEF.
- [30] For instance, ten X-ray structures of the 1918 HA have been determined and the H3 numbering was used for nine of them.
- [31] When  $n = 1$ , this is the coefficient of the component for residue  $j$ .
- [32] Two 1917 avian sequences were determined, but they are partial ones.
- [33] Being an eigenvector, a component is normalized, that is, the sum of the square of its coefficients is one.
- [34] H3 numbering.